Comparing a phased combination of acoustical radiosity and the image source method with other simulation tools

Gerd Marbjerg
Saint-Gobain Ecophon, 2650 Hvidovre, Denmark

Jonas Brunskog, Cheol-Ho Jeong
Acoustic Technology, Department of Electrical Engineering, Technical University of Denmark, 2800 Kgs. Lyngby, Denmark

Erling Nilsson
Saint-Gobain Ecophon, 265 03 Hyllinge, Sweden

Summary
A phased combination of acoustical radiosity and the image source method (PARISM) has been developed in order to be able to model both specular and diffuse reflections with angle-dependent and complex-valued acoustical descriptions of the surfaces. It is of great interest to model both specular and diffuse reflections when simulating the acoustics of small rooms with non-diffuse sound fields, since scattering from walls add to the diffuseness in the room. This room type is often seen in class rooms and offices, as they are often small rectangular rooms with most of the absorption placed on the ceiling. Here, PARISM is used for comparisons with other simulation tools and measurements. An empty, rectangular room with a suspended absorbing ceiling is used for the comparisons. It was found that including the phase information in simulations increases the spatial standard deviation, even if only the propagation phase is considered. It was furthermore found that it is difficult to match simulations with measurements, when the input data are unknown and therefore estimated.

PACS no. 43.55.Ka, 43.55.Br

1. Introduction

It is of great practical interest to predict the acoustics of small rectangular rooms with absorbing ceilings, since this room type is often seen in rooms such as classrooms and offices. In the present paper, this room type is used for comparisons of simulations using different room acoustic simulation tools with measurements.

A new simulation tool has been developed especially to be suitable for small rooms with absorbing ceilings. The model, Phased Acoustical Radiosity and the Image Source Method (PARISM), includes both specular and diffuse reflections considering phase information and angle-dependent boundary conditions.

The phase of a wave component depends on two things: the phase shifts on reflections in its reflection path and its propagation distance [1, 2]. To consider the phase on reflections, complex-valued boundary conditions are needed. The propagation phase can be considered even if the phase shifts on reflections are unknown.

Room acoustic simulation tools often disregard both the phase shifts on reflections and the propagation phase. This can be problematic when considering frequencies below the Schroeder frequency as the modal behaviour of the room has a large influence on the sound field and thus interference needs to be considered.

The present paper compares PARISM simulations with measurements and simulations from other tools.

2. Method

2.1. PARISM

As the name implies, PARISM combines the image source method (ISM) with acoustical radiosity (AR). In ISM, the reflections are specular and phased, whereas they are diffuse and without phase information in AR. The reflection pattern is assumed to follow Lambert's law [3]

$$I(\theta_{rad}) = I(0)\cos(\theta_{rad}), \quad (1)$$

where $I(0)$ is the intensity radiated in the normal direction of the surface and $I(\theta_{rad})$ is the intensity radiated in the direction which has the angle θ_{rad} with the normal of the surface. In AR, the surfaces are divided into elements and these elements function as both sources and receivers of radiation density. Radiation density is defined as the rate at which energy leaves a unit area of a surface. The result of AR is an energy impulse response from which a pressure impulse response is reconstructed by regarding AR as being stochastic [4, 5, 6]. Each realisation of the impulse response is considered as a member of the ensemble of possible impulse responses. For the calculation of energy-based room acoustical parameters, the squared expectation value of the ensemble is estimated.

In ISM, the source and image sources are seen as point sources. The total frequency response at the receiver is found as the sum of contribution from all image sources by [7, 8]

$$p(f) = \sum_{q=1}^{N_q} \frac{\mathrm{j}C_q(f)\mathrm{e}^{-\mathrm{j}kr_{Pq}}\mathrm{e}^{-\frac{m}{2}r_{Pq}}}{r_{Pq}}, \quad (2)$$

where N_q is the number of image source, C_q is the source factor of image source q, $k = 2\pi f/c_0$ is the wave number with c_0 as the speed of sound in air and f as the frequency, r_{Pq} is the distance between the source q and the receiver P and m is the power attenuation coefficient of air. C_q is found as [9]

$$C_q = \prod_{k=1}^{n_q} \{R_k(\theta_{Pk})\sqrt{1-s_k}\}, \quad (3)$$

where n_q is the number of reflection in the reflection path of q, s_k is the scattering coefficient of reflection k and $R(\theta_{kP})$ is the angle-dependent reflection coefficient of reflection k in the reflection path between the image source q and the receiver P. The determination of image sources is terminated once a predefined minimum of the source factor is reached. When the production of an image is terminated, the energy is transferred to AR [4, 5].

The pressure impulse response is found from ISM by inverse Fourier transform of the frequency response and is added to the reconstructed pressure impulse response from AR.

2.2. The other simulation tools

Two simulation tools are used for comparison with PARISM; ODEON and CARISM. CARISM [10] is, as PARISM, a combination of ISM and AR, but CARISM is an energy-based model. The ISM is therefore implemented in terms of energy rather than pressure. CARISM furthermore determines the energy impulse response assuming a flat frequency response, thus only for one absorption coefficient and scattering coefficient at a time. Such an energy impulse response can be seen as representing the energy impulse response for a frequency band.

ODEON is a hybrid tool in which early reflections are found by a combination of ISM and ray tracing, and the late reflections are found by ray tracing. Scattering in ODEON is modelled by vector based scattering, in which the resulting ray is calculated by weighting the specular direction and a random scattered direction by means of the scattering coefficient. The random scattered direction is found by a method of oblique Lambert [11].

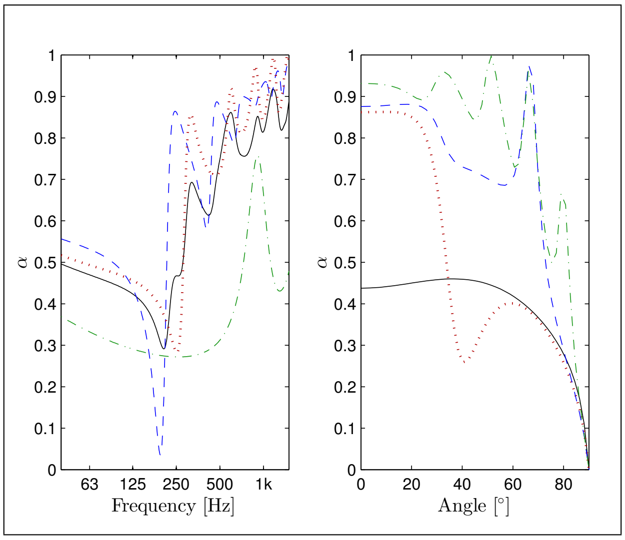

Figure 1. Absorption coefficients calculated by Komatsu's model. Flow resistivity: $\sigma = 12\frac{kPas}{m^2}$, thickness: $d = 50$ mm, gap: $d_0 = 75$ cm. *Left*: Absorption coefficients at different angles of incidence and the random incidence absorption coefficient. ——: Random incidence; ········: 45°; – – – : 0°; -·-·-·- : 79°. *Right*: Absorption coefficients as a function of angle of incidence. ——: 125 Hz; ········: 250 Hz; – – – : 500 Hz; : 1 kHz.

2.3. The example room

For the investigation, a rectangular room (7.32 x 7.57 x 3.5 m) with a suspended absorbing ceiling has been chosen. The ceiling is a porous absorber with a thickness of $d = 50$ mm and the gap behind it is $d_0 = 75$ cm. The resulting height of the room is therefore 2.7 m. The impedance of the ceiling is modelled using Komatsu's model [12] with a flow resistivity of $12\frac{\text{kPas}}{\text{m}^2}$. If extended reaction is assumed, the plane wave reflection coefficient, $R(\theta, f)$, for an infinitely large surface with surface impedance $Z(\theta, f)$ can be found as [8]

$$R(\theta, f) = \frac{Z(\theta, f) - \rho_0 c_0/\cos\theta}{Z(\theta, f) + \rho_0 c_0/\cos\theta}, \quad (4)$$

where θ is the angle of incidence with respect to the normal of the surface and ρ_0 is the density of air. The absorption coefficient is related with the reflection coefficient by $\alpha = 1 - |R|^2$. The absorption coefficient of the ceiling can be seen in Figure 1. CARISM and ODEON need angle independent absorption coefficients as input. Therefore Paris' law [13] is used to obtain the random incidence absorption coefficient, which can also be seen in Figure 1. To obtain the absorption coefficient in octave bands, the average of the random incidence absorption coefficient is taken within each band. The result of this is seen in Table I denoted as α_{ceil}. A simulation with PARISM using the random incidence absorption coefficient of the ceiling is also done. In this simulation, angle dependence and phase shifts on reflections from the ceiling are disregarded, but the propagation phase is still included in the ISM part of PARISM.

Table I. Absorption coefficients. α_{ceil} of the ceiling and α_{surf} of the other 5 surfaces in octave bands with centre frequencies, f_c.

f_c [Hz]	63	125	250	500	1000
α_{surf}	0.075	0.057	0.046	0.035	0.036
α_{ceil}	0.47	0.42	0.46	0.75	0.84

Table II. Receiver positions, P_1 to P_6, in the example room.

P_1	[1.51, 3.88, 1.2] m	P_2	[4.03, 4.10, 1.2] m
P_3	[3.37, 2.50, 1.2] m	P_4	[5.74, 2.90, 1.2] m
P_5	[2.10, 1.18, 1.2] m	P_6	[5.74, 6.27, 1.2] m

For the simulations, the room is modelled as a rectangular box with 6 surfaces, but the actual room has has different materials on the floor and the walls, and has windows and doors. The acoustic properties of the actual surface materials are however unknown and the absorption coefficients are therefore estimated. This is done by applying Sabine's equation to measurements of the reverberation time done in the room without the absorbing ceiling installed, thus obtaining an average absorption coefficient. This can be found in Table I denoted as α_{surf}. The ISM part of PARISM needs reflection coefficients for a continuous frequency vector instead of octave bands values. The reflection coefficients are therefore determined by linear interpolation and taking the square root. The room being empty, the scattering coefficient in is expected to be low and is therefore set to 0.05 for all surfaces and frequencies. The Schroeder frequency of the room is approximately 180 Hz.

The source is located in [3.69, 6.45, 1.5] m and six receiver positions are considered, as seen in Table II.

Results will be regarded in terms of the room acoustical parameters reverberation time T_{30} and early decay time EDT, as defined by the ISO standard 3382-1 [14] along with comparisons of decay curves.

3. Results

Figure 2 compares PARISM results using the reflection coefficient for the ceiling with PARISM results using the random incidence absorption coefficient and measurement results. Hereafter, the term PARISM results always refers to PARISM simulations using the reflection coefficient for the ceiling. When looking at the measurement results, a dip in reverberation time and early decay time is observed at 250 Hz. Therefore, a peak in the absorption coefficient of the ceiling should be expected in this frequency range. When looking at Figure 1, it is seen that the opposite is predicted by Komatsu's model. Neither a dip nor a peak is seen in the PARISM and random incidence PARISM results. When comparing the random incidence PARISM results for EDT with the PARISM results for EDT, it is seen that the reflection coefficient performs best at 63 Hz and 125 Hz, whereas the random incidence absorption coefficient performs better at 500 Hz and 1 kHz. There are in fact large deviations between EDT of the PARISM results and the measurements at 500 Hz and 1 kHz. It can be seen in Figure 1 that the absorption coefficients at 500 Hz and 1 kHz fluctuate greatly as a function of the angle with peaks at high angles of incidence. When using the complex-valued and angle-dependent reflection coefficient in PARISM, the model is very sensitive to input data, and if the determination of the reflection coefficient is not correct, it can lead to errors in the results. Using angle-dependent surface description also makes the model very sensitive to the changes in the scattering coefficient. It is possible that the scattering coefficient is underestimated at high frequencies. Using the random incidence absorption coefficient is however a more robust method.

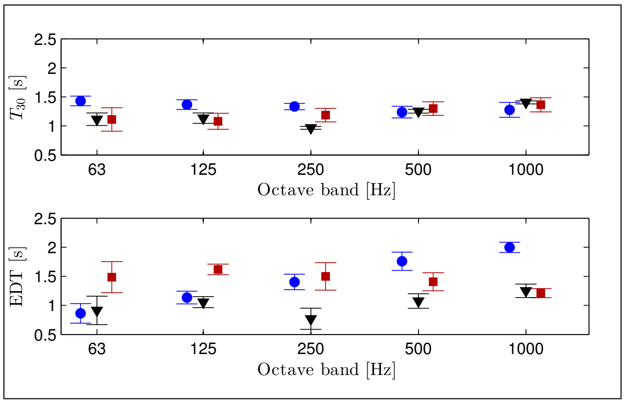

Figure 2. Results in terms of T_{30} and EDT with the spatial standard deviation. ●: PARISM; ▼: Measurement; ■: PARISM with random incidence absorption coefficient used for the ceiling.

Figure 3 compares PARISM results with ODEON and measurement results, and Figure 4 compares PARISM results with CARISM and measurement results. For both the ODEON and the CARISM results, the spatial standard deviation is lower than those of the measurements and the PARISM simulations. This is due to the fact that ODEON and CARISM are energy-based models that do not consider the phase of neither propagation nor phase shifts on reflections, thus disregarding interference. When the interference is disregarded, the simulations are less sensitive to the observation point. For all frequencies except 250 Hz, ODEON underestimates T_{30} and EDT. It is probable that this is due to the use of the random incidence absorption coefficient, as this often overestimates the absorption at high angles of incidence.

An unexpected observation can be made when regarding the CARISM results in Figure 4, as T_{30} is lower than EDT for all frequencies. In a rectangular room with most absorption on the ceiling, the opposite is expected. The sound field in such a room can be seen as split in two parts: one parallel and one perpendicular to the absorbing ceiling. The parallel field has angles of incidence close to 90° with respect to the normal direction of the surface and is therefore denoted the grazing sound field. The perpendicular sound field is denoted the non-grazing sound field. Since the absorption coefficient of the ceiling is often low at high angles of incidence, the non-grazing sound field will decay faster than the grazing sound field, making the total decay non-exponential. The fast decay will dominate

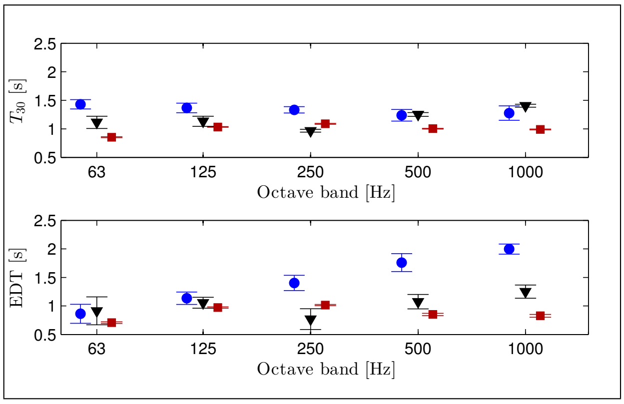

Figure 3. Results in terms of T_{30} and EDT with the spatial standard deviation. ●: PARISM; ▼: Measurement; ■: ODEON.

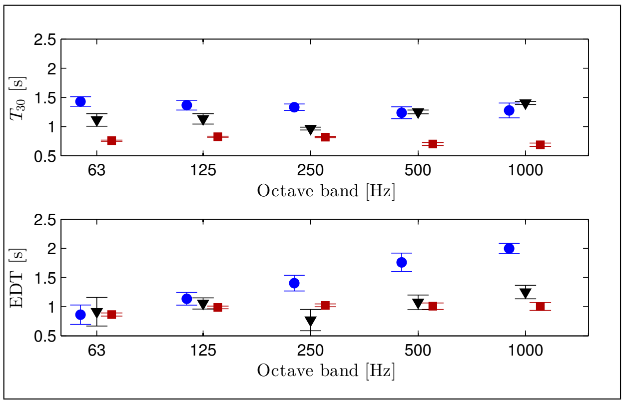

Figure 4. Results in terms of T_{30} and EDT with the spatial standard deviation. ●: PARISM; ▼: Measurement; ■: CARISM.

the early part of the decay curve and the slower decay will dominate the late part of the decay curve, thus giving an EDT that is lower than T_{30} [15].

To investigate why the EDT values are higher than the T_{30} values for the CARISM simulations, the decay curves are plotted for the measurement results, the PARISM results, the random incidence PARISM results and the CARISM results. 50 dB decay curves are plotted for the 63 Hz, 250 Hz and 1 kHz octave bands in Figure 5. It can clearly be seen from the figure that there are breaks in the decay curves of the CARISM results a little after 0.2 s and in the decay curves of the PARISM results around 0.7 s. This is probably where termination of the production of image sources begins, as it can also be observed that the curves become smoother after these breaks. The smoothness and slope are increased, since the energy of a terminated image source is thereafter assumed to be diffusely reflected, thus increasing the overall diffuseness of the sound field. The decay curves of PARISM and CARISM seem to match the measured decay curves better before the termination of the image sources, which indicates that the image sources are terminated too quickly. This is why EDT is higher than T_{30} for the CARISM results and it would be expected that an increase in the amount of image sources would greatly improve the results. As the break can be observed after around 25-30

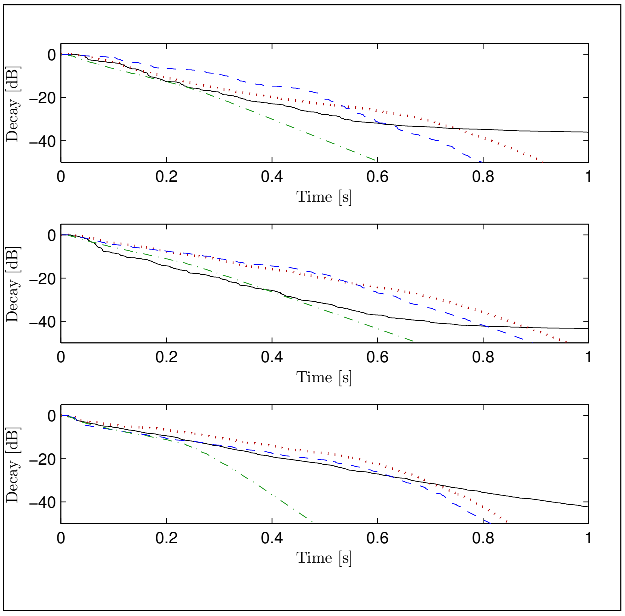

Figure 5. Decay curves. *Above*: 63 Hz octave band. *Middle*: 250 Hz octave band. *Below*: 1 kHz octave band. ——: Measurement; ·······: PARISM; – – –: PARISM with random incidence absorption coefficient used for the ceiling. ; –·–·–: CARISM.

dB decay for the PARISM results, T_{30} is also expected to be influenced by the termination of image sources for the PARISM results. These observations show that it is of great importance to consider a sufficient amount of specular reflections in the present room type.

A closer look is now taken at the early part of the decay curves, see Figure 6. For the 63 Hz octave band, it is seen that the PARISM decay curve matches best with the measured one. The CARISM decay curve decays faster than ones of the measurement, the PARISM simulation and the random incidence PARISM simulation. The same can be observed at the 250 Hz octave band, however not as significantly. The reason why this can be observed is that CARISM assumes a flat frequency response over all frequencies, whereas the results from PARISM and the measurements are filtered in octave bands and thus are bandlimited results. The effect is stronger for the lower frequency bands as these are narrower and thus contain less modes within each band.

At 1 kHz in Figure 6, it seen that the PARISM results decay slower than the measurement results in the first 10 dB. This is reflected in the overestimation of the EDT of the PARISM results at 500 Hz and 1 kHz, as can be seen in Figures 2 to 4. It was suggested that the deviations could be due to an underestimation of the scattering coefficient. A simulation is therefore done with a scattering coefficient of 0.1 in PARISM. The decay curves for the 500 Hz and 1 kHz octave bands are shown in Figure 7, where it is seen that the decay curve of PARISM with the higher scattering coefficient matches the one of the measurements better than that of PARISM with the lower scattering coefficient. This indicates that the higher scattering coefficient is closer to the actual scattering at these frequencies. As

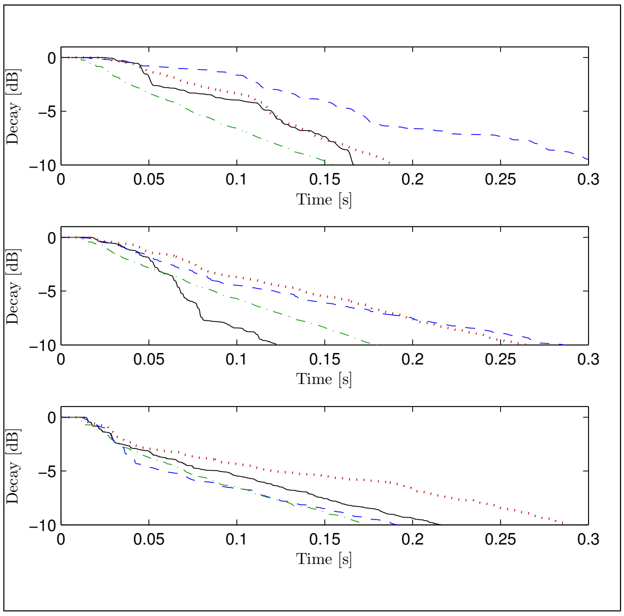

Figure 6. Decay curves. *Above*: 63 Hz octave band. *Middle*: 250 Hz octave band. *Below*: 1 kHz octave band. ——: Measurement; ·······: PARISM; – – – : PARISM with random incidence absorption coefficient used for the ceiling. ; -·-·-: CARISM.

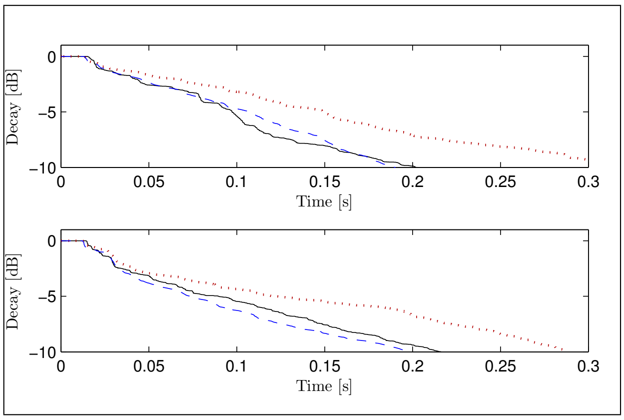

Figure 7. Decay curves. *Above*: 500 Hz octave band. *Below*: 1 kHz octave band. ——: Measurement; ·······: PARISM with a scattering coefficient of 0.05; – – – : PARISM with a scattering coefficient of 0.1.

the surfaces of the room are not completely smooth but include doors and windows, it is reasonable to assume that the scattering at higher frequencies is higher than at low frequencies.

In Figure 6, it is observed that there are details in the very early part of the measured decay curves which are not seen in the ones predicted by PARISM, especially at low frequencies. As mentioned in Section 2.1, the pressure impulse response of AR is reconstructed by considering AR as being stochastic, leading to an ensemble of realisations. For the determination of room acoustical parameters, the squared expectation value of this ensemble is estimated. In all results shown previously from PARISM, the squared expectation value has been used. If the statistical assumptions behind the reconstruction of the AR

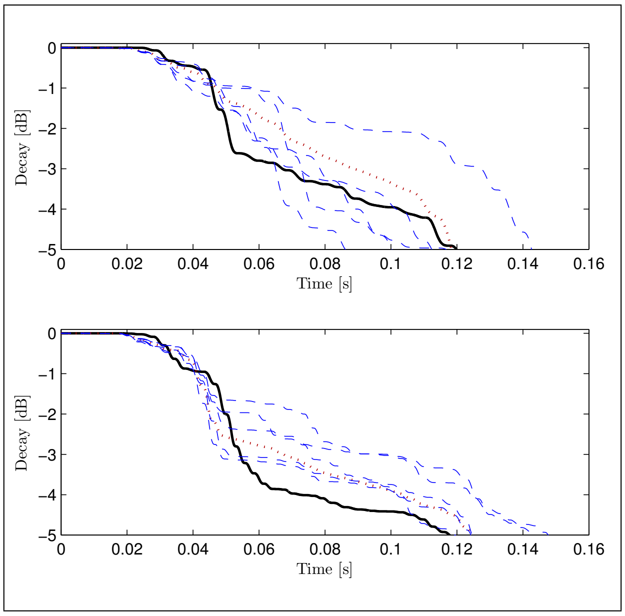

Figure 8. Decay curves. *Above*: 63 Hz octave band. *Below*: 125 Hz octave band. ——: Measurement; ·······: PARISM, ensemble mean of squared impulse response; – – – : Five PARISM decay curves determined with five different realisations the pressure impulse response from AR.

impulse response are correct, a member of the ensemble of realisations of the impulse response should result in a total pressure impulse response matching the measurement. Figure 8 shows the decay curves for the 63 Hz and 125 Hz octave bands with five different realisations of the AR pressure impulse response along with the expectation value and the measured decay curve. It is seen that none of the realisations match the measured decay curve precisely, but some come closer than the expectation value. This indicates that the statistical assumptions behind the reconstruction of the pressure impulse response are valid. Five realisations are however not enough to neither prove nor reject the validity completely. There are furthermore uncertainties in the energy impulse response used for the reconstruction, which can also influence the reconstructed pressure impulse response.

4. Discussion

PARISM is a model with the ability to include detailed descriptions of the surfaces, making it sensitive to the input parameters. This can be problematic as precise input parameters are often difficult to obtain. In the present example all input parameters are estimated. The reflection coefficient of the ceiling is determined by Komatsu's model and by assuming that it can be seen as an infinite absorber on which plane waves are incident. This is however not completely true for an absorbing ceiling installed in a room. The absorption coefficients of the other surfaces are estimated by assuming that they can be described by an average for all surfaces. This average is furthermore found on the basis of measured reverberation times and Sabine's equation, thus assuming that the sound field in the room without an absorbing ceiling is diffuse.

The scattering coefficient is also an estimate, and is assumed to be equal for all surfaces and frequencies. The room type of the present example is very sensitive to surface scattering [16]. The PARISM results confirmed this, and it was seen that a frequency-independent scattering coefficient can be insufficient to describe the scattering surface properties.

With the above mentioned assumptions, it is difficult to determine which of the simulation tools gives the best results. It is however clear that there are significant differences between the results from the simulation tools. Low spatial standard deviations were observed in the results of the energy-based simulation tools ODEON and CARISM, compared to the spatial standard deviations of the measurement results and the PARISM results. This indicates that there are details in the sound field that are not captured by the energy-based tools and that these therefore are better for predicting an average of the room rather than differences between observation points. The results from the random incidence PARISM simulations also had high spatial standard deviation, showing that even if the phase of a boundary condition is unknown, the propagation phase can still have an influence on the prediction of the sound field.

5. Concluding remarks

The new model PARISM has been compared with other room acoustical simulation tools. It was shown that significant differences were seen between the methods. All simulation tools were compared with measurements, but it was seen that matching measurements is difficult when the input parameters to the simulation tools are unknown and therefore must be estimated. For better comparisons and validation of PARISM, better input data is therefore needed.

It was also shown that the amount of image sources included in the prediction on the impulse response has a great influence of the results of PARISM and CARISM. The interruption criterion therefore also needs further investigations.

Acknowledgement

The authors would like to thank Alejandro Gonzalez Pacheco for carrying out the measurements, which were used for the comparisons. This project is financially supported by the Innovation Fond Denmark.

References

[1] B. Yousefzadeh, M. Hodgson: Energy- and wave-based beam tracing prediction of room-acoustical parameters using different boundary conditions. J. Acoust. Soc. Am. **132** (2012) 1450–1461.

[2] C.-H. Jeong: Absorption and impedance boundary conditions for phased geometrical-acoustics methods. J. Acoust. Soc. Am. **132** (2012) 2347–2358.

[3] E.-M. Nosal M. Hodgson and I. Ashdown: Improved algoritms and methods for room sound-field prediction by acoustical radiosity in arbitrary polyhedral rooms. J. Acoust. Soc. Am. **116** (2004) 970–980.

[4] G. Marbjerg, J. Brunskog, C.-H. Jeong, E. Nilsson: Description and validation of a combination of acoustic radiosity and the image source method. Proc. 2014 Forum Acusticum.

[5] G. Marbjerg, J. Brunskog, C.-H. Jeong, E. Nilsson: Description and validation of a phased combination of acoustical radiosity and the image source method. *Submitted for publication*.

[6] A. Le Bot and A. Bocquillet: Comparison of an integral equation on energy and the ray-tracing technique in room acoustics. Build. Acoust. **11** (2004) 39–60.

[7] J. B. Allen and D. A. Berkley: Image method for efficiently simulating small-room acoustics. J. Acoust. Soc. Am. **65** (1979) 943–950.

[8] F. Jacobsen, P. M. Juhl: Fundamentals of General Linear Acoustics. Wiley, 2013, p. 47.

[9] F. P. Mechel: Improved mirror source method in room acoustics. J. Sound Vib. **256** (2002) 873–940.

[10] G. I. Koutsouris, J. Brunskog, C.-H. Jeong, F. Jacobsen: Combination of acoustical radiosity and the image source method. J. Acoust. Soc. Am. **133** (2013) 3963–3974.

[11] C. L. Christensen, G. Koutsouris: Odeon Room Acoustics Program, Version 12, User Manual, Industrial, Auditorium and Combined Editions. Odeon A/S, Lyngby, Denmark, 2013.

[12] T. Komatsu: Improvement of the Delany-Bazley and Miki models for fibrous sound-absorbing materials. Acoust. Sci. & Tech. **29** (2008) 121–129.

[13] E. T. Paris: On the coefficient of sound-absorption measured by the reverberation method. Phil. Mag. **5** (1928) 489–497.

[14] ISO standard 3382-1 - Measurement of room acoustic parameters - Part 1: Performance spaces. International Organization for Standardization, Geneva, Switzerland (2009).

[15] E. Nilsson: Decay processes in rooms with non-diffuse sound fields - Part I: Ceiling treatment with absorbing material. Build. Acoust. **11** (2004) 39–60.

[16] E. Nilsson: Decay processes in rooms with non-diffuse sound fields. Part II: Effect of irregularities. Build. Acoust. **11** (2004) 133–143.